Vol 17 No 4, April 2008
1674-1056/2008/17(04)/1467-05

Chinese Physics B

© 2008 Chin. Phys. Soc.
and IOP Publishing Ltd

Field emission characteristics of nano-sheet carbon films deposited by quartz-tube microwave plasma chemical vapour deposition

Gu Guang-Rui(顾广瑞)[a)†], Jin Zhe(金 哲)[a)], and Ito Toshimichi[b)]

[a)] *Department of Physics, College of Science, Yanbian University, Yanji* 133002, *China*
[b)] *Division of Electrical, Electronic and Information Engineering, Graduate School of Engineering, Osaka University, Osaka* 565-0871, *Japan*

(Received 8 July 2007; revised manuscript received 22 October 2007)

Nano-sheet carbon films are prepared on Si wafers by means of quartz-tube microwave plasma chemical vapour deposition (MPCVD) in a gas mixture of hydrogen and methane. The structure of the fabricated films is investigated by using field emission scanning electron microscope (FESEM) and Raman spectroscopy. These nano-carbon films are possessed of good field emission (FE) characteristics with a low threshold field of 2.6 V/μm and a high current density of 12.6 mA/cm^2 at an electric field of 9 V/μm. As the FE currents tend to be saturated in a high E region, no simple Fowler–Nordheim (F–N) model is applicable. A modified F–N model considering statistic effects of FE tip structures and a space-charge-limited-current (SCLC) effect is applied successfully to explaining the FE data observed at low and high electric fields, respectively.

Keywords: field emission, carbon films, nano-sheet, microwave plasma chemical vapour deposition
PACC: 7970, 6146

1. Introduction

In recent years, a great effort has been made to develop electron field emitters for the application in display products.[1−3] Much attention has been paid to carbon-based emitters, such as diamond,[4] diamond-like carbon,[5] carbon nanotubes,[6,7] and amorphous carbon (A–C),[8] and so on, because these materials have good chemical, electrical, optical, and mechanical properties. In order to obtain good field emission properties at a low threshold voltage and a high current density, it may be essential to fabricate nano-structured carbon films. Various nano-structured carbon films have been investigated recently. Zhang *et al*[9] reported that the low threshold field of carbon nanotubes was attributed to the random distribution which brought on the high geometric enhancement factor. Wang and co-workers found that the good field emission properties of carbon nano-sheets[10] and carbon nanoflakes[11] might be due to the high density of graphite edges with potential emission sites. The research results given by wang *et al*[12] indicated that the carbon nanocones with a great aspect ratio had a higher emission current and a lower threshold field. The field emission properties of other nano-carbon films have been studied, too.[13,14]

Recently, many studies have indicated that the F–N curves of nano-structured carbon films manifest themselves the non-linearity.[9,15,16] This phenomenon cannot be reasonably explained by the classic F–N theory. The F–N theory should be adapted to flat cathode surfaces of metals with a sufficient number of free electrons. Thus, it may not be applicable for various carbon films that have complex structures with irregular shapes where the emission sites and electrical conductivity are significantly different from those of pure metal plates. Moreover, the number of FE sites may not be constant when the electrical field varies in a wide range where the maximum local field reaches an extremely high field of 10^7V/cm. Therefore, it may be necessary to modify the F–N theory for solving the above problem. We have proposed a modified F–N model considering statistical distribution of field emission tip structures and explained successfully the field emission mechanism of carbon nano-films.[17,18]

In the present study, we fabricate nano-sheet carbon films on Si substrates by means of the quartz-tube MPCVD and report further evidences for our modified

†E-mail: grgu@byu.edu.cn

F–N approach and a possible FE current saturation mechanism.

2. Experiment

Carbon films were deposited on Si substrates by means of quartz-tube MPCVD in a mixture of CH_4 (5sccm) and H_2 (20sccm) at a reactive pressure of 8×10^3 Pa and a microwave plasma (MP) power of 450W. The chamber base pressure was below 1.3×10^{-4} Pa and the deposition time was 3 h. Si substrates were ultrasonically scratched with diamond powder prior to the deposition process (such a treatment is commonly employed as a standard method of enhancing nucleation for diamond films.[19]) Furthermore, a 10-min pretreatment with H_2 plasma irradiation was carried out at a reactive pressure of 4×10^3 Pa and an MP power of 300 W for the scratched Si surfaces in a quartz-tube reaction chamber.

Surface morphologies of the carbon films were observed by an FE scanning electron microscope. The structures of the carbon films were characterized by Raman spectroscopy. The FE testing was performed in a high vacuum ($< 6.6\times10^{-4}$Pa) system at room temperature. A film sample (2mm×5mm) acted as a cathode while an aluminium plate was utilized as an anode. The anode was set to be 100 μm away from the sample surface with two 50 μm-thick Teflon sheets used as a spacer. Macroscopic electric fields ranging from 0 to 9V/μm were applied across the anode and cathode separately.

3. Results and discussion

A typical FESEM image of a typical carbon film deposited in the present study is shown in Fig.1(a), and its corresponding magnifications are shown in Figs.1(b) and 1(c). These pictures indicate that the film surface is composed mainly of stand-up nanostructured carbon sheets which are complicatedly twisted with each other. This kind of structure is little different from that of other nano-sheets.[10] The SEM

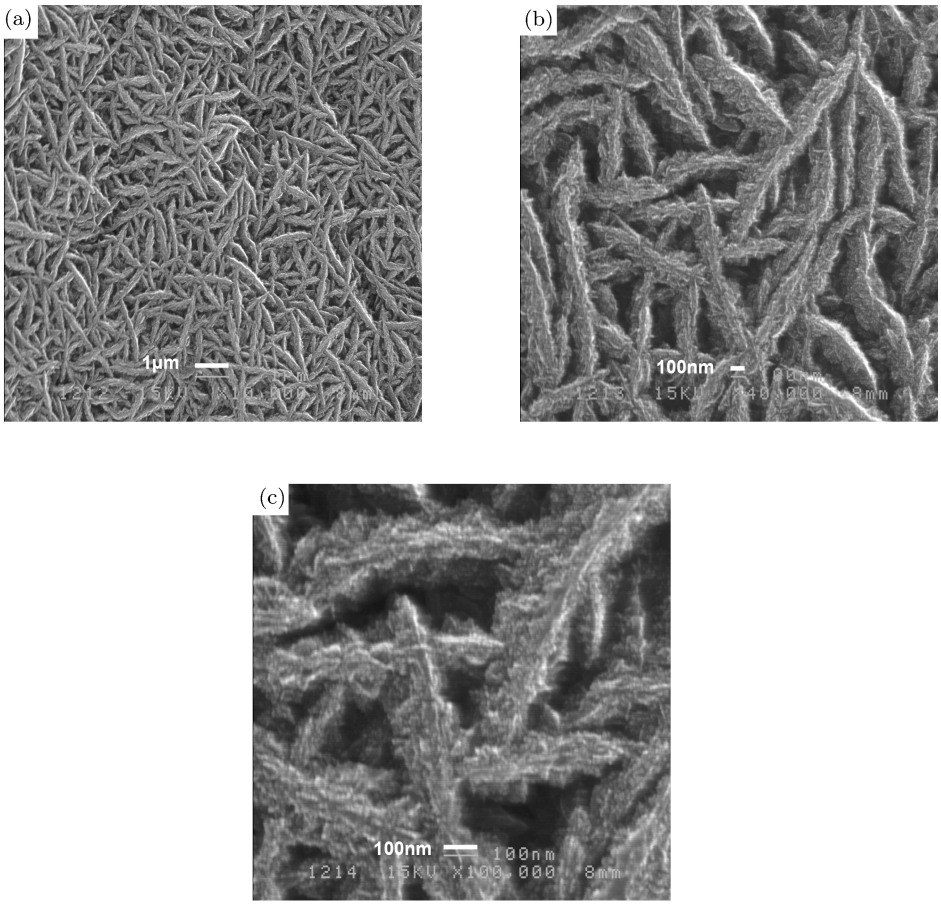


Fig.1. FESEM images taken from a typical carbon film grown on a Si substrate by using quartz-tube microwave plasma CVD. Subfigures (b) and (c) are parts of magnified area of subfigure (a).

images look like veins with about 100 nm in width and 1–3 μm in length. Moreover, many nano-protuberances are observed on the surface of nano-sheets, so a large number of potential field emission sites can be expected to be formed on the nano-carbon films.[10] As shown in Fig.2, Raman spectra taken from the nano-carbon film have two Raman peaks located at about 1353 cm^{-1} and 1587 cm^{-1} separately, indicating that standard features are formed in the carbon films.

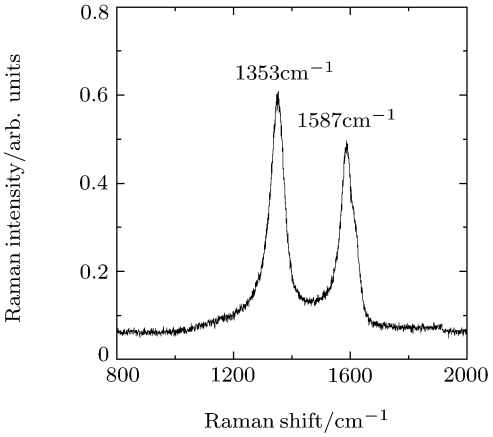


Fig.2. Raman spectrum taken from the carbon film shown in Fig.1.

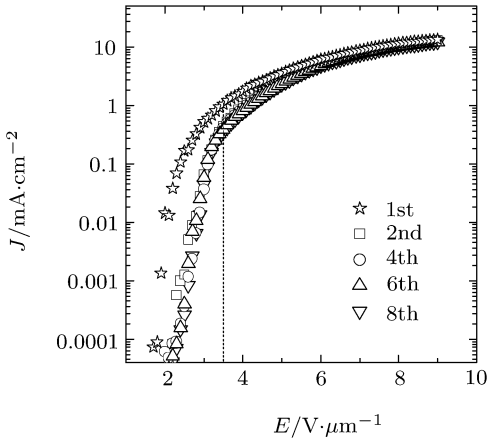


Fig.3. Field emission current density J versus macroscopic electric field ($J-E$) for the 1st, 2nd, 4th, 6th and 8th measurements on the carbon film shown in Fig.1.

The values of FE current density (J) are measured several times as a function of the macroscopic electric field (E) for as-grown samples of nano-carbon sheets, and they are shown in Fig.3. It is indicated that an unstable emission with little high FE current is obtained for the first measurement and that the reproducibility and the stability of the $J-E$ data both are improved significantly through increasing the measurement times. The average threshold E of 2.6 V/μm at a current density of 10 μA/cm^2 is substantially lower than those for other carbon nano-sheets[10] and carbon nanotubes,[20] and the value of J increases with increasing E at $E < 3$ V/μm, above which there occurs an obvious saturation behaviour of J. The average current density of 12.6 mA/cm^2 is obtained at E=9 V/μm.

In order to fully understand the FE mechanism, the FE data are discussed first in a low E region ($E < 3.5$ V/μm) where the saturation tendency of J is not found. So a modified F–N model considering the statistical distribution in structure of the FE tips and E-dependent parameters is presented as follows:[17,18]

$$\ln\frac{J}{E^2} = \ln\left(\frac{1.5414\times10^{-6}S\beta^2}{\varphi}\right) - \frac{6.8309\times10^{9}\varphi^{3/2}}{\beta}\left(\frac{1}{E}\right), \qquad (1)$$

where J (in A/m^2) is the emission current density, E (in V/m) is the applied electric field, β is the effective field enhancement factor, S is the effective relative emission area and φ (in eV) is the work function.

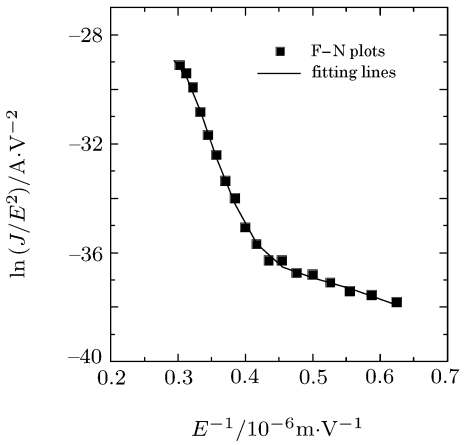


Fig.4. F–N relation at low electric fields ($E < 3.5$V/μm) for the 4th measurement, denoted with a set of short lines fitted by using a local fitting method with E-dependent parameters of the effective field enhancement factor and the effective relative emission area.

Here, the work function φ is assumed to have a constant value of 4.5 eV, S and β are assumed to change with E while they are regarded as constant values in each E sector of about 0.1V/μm. As shown in Fig.4, the 4th measurement F–N data in the low E region are fitted in each sequential 0.1 V/μm E region by using a locally fitting method, indicating reasonably good agreement between the results obtained from the experiment and the modified F–N model.

The parameters S and β are evaluated from the locally fitting process as a function of E in a range

from 2.0 to 3.5 V/μm, and they are shown in Fig.5. It is found that the β value decreases first at relatively low values of E and then increases at relatively high values of E with E value increasing. The β value is more than 9320 at the low field edge of 2.0 V/μm, and minimum β value is about 820 at 3.0 V/μm. The higher β value can be attributed to quite a number of nano-protuberances on the surface of nano-sheets. The S value increases first at relatively low values of E and then decreases at relatively high values of E with E value increasing. The S value is around 1×10^{-17} when the value of E is 2.0 V/μm and a maximum value of S is about 0.05 at 3.0 V/μm. Furthermore, the deduced S values are extremely small, suggesting that the effective emission areas of the samples are much smaller than their apparent surface areas.

The variations of S and β with E can be understood as follows. In a low E region, when an extremely low E is applied to the sample, the emission behaviour is governed by the FE sites with a larger value of β whereas the contribution to J from FE sites with a smaller value of β is neglected. When E value is further increased to a relatively large value, FE sites with a smaller value of β turn to making a contribution to J. The number of such sites with smaller values of β should be significantly larger than that of the sites with larger values of β. In the low E region, the FE currents from such low β sites significantly increase with the value of E increasing while the contribution to J from the larger β sites relatively decreases due to such a saturation effect as observed in the case of sufficiently high J.

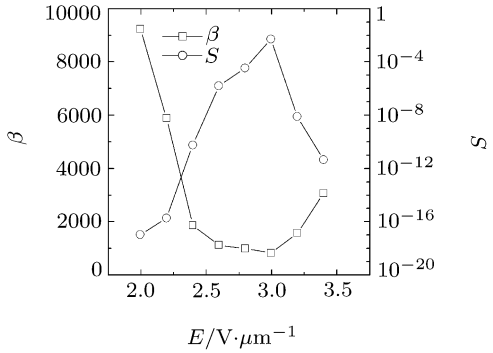


Fig.5. The effective field enhancement factor, β, and the effective relative emission area, S, deduced from the local fitting procedure as a function of the macroscopic electric field, E.

As shown in Fig.4, at $E > 3.0$ V/μm, S again becomes smaller with the value of E increasing. This cannot be explained reasonably in terms of the present modified F–N model. On the one hand, the FE current density should be limited by the density of states near the Fermi energy for C atoms located at the emitter tips such as carbon nanotubes,[21] and on the other hand, the value of φ for the emitter tip surface may be E-independent.[22] Furthermore, each FE emitter that gives the field enhancement effect may not work fully at such a high E due to an insufficient screening effect by the limited number of free electrons.

Thus, in the high E region, a substantial contribution of some kind of space-charge-limited-current (SCLC) mechanism may be considered to be able to explain the FE behaviour measured in the sufficiently high E region, namely at E larger than about 6 V/μm. In such a case, J in the saturated region may be represented in terms of the Child–Langmuir law[23] as follows:

$$J \propto E^{3/2}. \tag{2}$$

As a matter of fact, the measured FE data in the high E region can be well fitted only at E larger than about 6 V/μm by using the above equation as shown in Fig.6. This means that the SCLC model may be a strong candidate for the physical mechanism explaining the saturated behaviour in FE currents. Thus, the FE currents in the middle of E region may be controlled by both the F–N model and the SCLC model. A further study on this issue is needed.

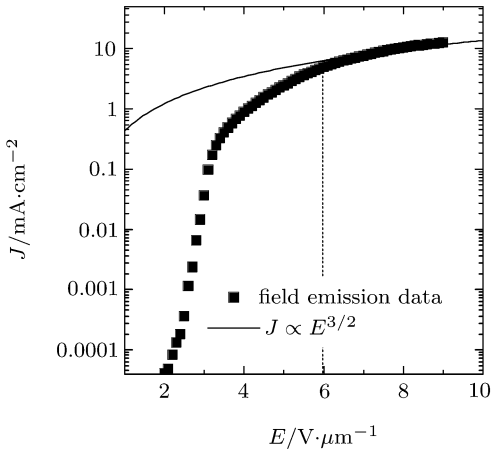


Fig.6. $J-E$ data of the 4th measurement for the carbon film with a curve fitted as $J \propto E^{3/2}$ in terms of the Child–Langmuir space-charge-limited-current model.

4. Conclusions

Nano-sheet carbon films are successfully prepared on Si substrates by quartz-tube MPCVD. The good FE characteristics with a low threshold field of

2.6 V/μm and a high field emission current density of 12.6 mA/cm^2 are obtained from such films. The measured FE data are separately discussed both in a low E region and in a high E region. It is proposed that the modified F–N model considering the statistic effects in the low E region ($E < 3\,\mathrm{V}/\mu\mathrm{m}$) and the SCLC model in the high E region ($E > 6\,\mathrm{V}/\mu\mathrm{m}$) be able to explain the observed FE data. The present modified F–N model suggests that the effective field enhancement factor decreases while the relative emission area increases with the value of E increasing in the low E region. The FE behaviour observed in the high E region can be well reproduced in terms of the Child–Langmuir SCLC mechanism.

References

[1] Chen L, Zhang G M ,Wang M S and Zhang Q F 2005 *Chin. Phys.* **14** 181

[2] Song J H, Zhang G M, Zhang Z X, Sun M Y and Xue Z Q 2004 *Acta Phys. Sin.* **53** 4392 (in Chinese)

[3] Ma Y P and Wang M 2007 *Acta Phys. Sin.* **56** (in Chinese)

[4] Yuan G, Guo D B, Gu C Z, Dou Y and Song H 2007 *Acta Phys. Sin.* **56** 143 (in Chinese)

[5] Ye F, Xie E Q, Li R S, Lin H F, Zhang J and He D Y 2005 *Acta Phys. Sin.* **54** 3935 (in Chinese)

[6] Song L, Liu S, Zhang G M, Liu L F, Ma W J, Liu D F, Zhao X W, Luo S D, Zhang Z X, Xiang Y J, Shen J, Zhou J J, Wang G and Zhou W Y 2006 *Chin. Phys.* **15** 422

[7] Guo D B, Wang Q, Yuan G, Gu C Z and Song C H 2007 *Acta Phys. Sin.* **56** (in Chinese)

[8] Lu Z L ,Wang C Q, Jia Y, Zhang B L and Yao N 2007 *Chin. Phys.* **16** 843

[9] Zhang Y B, Lau S P, Huang L and Tanemura M 2005 *Appl. Phys. Lett.* **86** 123115

[10] Wang J J, Zhu M Y, Outlaw R A, Zhao X, Manos D M, Holloway B C and Mammana V P 2004 *Appl. Phys. Lett.* **85** 1265

[11] Wang J J, Zhu M Y, Zhao X, Outlaw R A, Manos D M, Holloway B C, Park C, Anderson T and Mammana V P 2004 *J. Vac. Sci. Technol.* B **22** 1269

[12] Wang W H, Lin Y T and Kuo C T 2005 *Diamond Relat. Mater.* **14** 907

[13] Gu G R, Wu B J, Jin Z and Ito T *Chin. Phys.* (Accepted)

[14] Tanemura M, Tanaka J, Itoh K, Fujimoto Y, Agawa Y, Miao L and Tanemura S 2005 *Appl. Phys. Lett.* **86** 113107

[15] Li J J, Gu C Z, Wang Q, Xu P, Wang Z L, Xu Z and Bai X D 2005 *Appl. Phys. Lett.* **87** 143107

[16] Srivastava S K, Vankar V D, Rao D V S and Kumar V 2006 *Thin Solid Films* **515** 1851

[17] Wang J Y and Ito T 2007 *Diamond Relat. Mater.* **16** 364

[18] Wang J Y and Ito T 2007 *Diamond Relat. Mater.* **16** 589

[19] Jiang N, Nishimura K, Shintani Y and Hiraki A 2003 *J. Cryst. Growth* **255** 102

[20] Bonard J M, Kind H, Stöckli T and Nilsson L O 2001 *Solid State Electron.* **45** 893

[21] Bonard J M, Stöckli T, Maier F, Heer W A D and Châtelain A 1998 *Phys. Rev. Lett.* **41** 1441

[22] Zheng X, Chen G H, Li Z, Deng S and Xu N 2004 *Phys. Rev. Lett.* **92** 106803

[23] Child C D 1911 *Phys. Rev.* **32** 492

Langmuir I 1921 *Phys. Rev.* **21** 419